Int J Fract (2012) 178:215–232
DOI 10.1007/s10704-012-9776-1

ORIGINAL PAPER

A damage-based temperature-dependent model for ductile fracture with finite strains and configurational forces

N. Van Goethem · P. Areias

Received: 29 December 2011 / Accepted: 12 October 2012 / Published online: 2 November 2012

Abstract In this paper we assess a crack propagation criterion based on the notion of configurational force in the spirit of Gurtin (Configurational forces as basic concepts of continuum physics. Applied mathematical sciences. Springer, Berlin, 2000). We extend the theory of Gurtin to finite strain elasto-plastic fracture and in addition take thermal effects into account. The global model is a system of nonlinear and non-smooth equations which are solved directly with a finite element discretization. Comparison with laboratory experiments is provided, thereby showing that the concept of configurational force can be successfully used for computational damage-based fracture tests on ductile materials.

Keywords Ductile fracture · Plasticity · Finite strains · Configurational forces · Thermal stress

1 Introduction

Damage (Lemaitre 1996) and fracture (Barenblatt 1959) are almost always intimately linked together in the available models for crack propagation coexisting in the literature. For instance, in Allaire et al. (2011) a damage model is shown to provide crack-like results in some limit case while in Bourdin et al. (2008) (see also Bourdin et al. 2011) a purely fracture-dedicated theoretical model is implemented numerically with help of an auxiliary variable which has the effect of smearing the crack. In principle, damage must be understood as an internal (here, scalar) thermodynamical variable ζ, which is therefore not necessarily measurable but whose interaction with other mechanical and/or defect variables has visible effects. In the present model, damage is rather a model parameter determining when crack will propagate: at a certain threshold the damage value is such that softening of the material is unbearable without propagation of the crack tip. Let us remark that damage can be cast within purely elastic brittle fracture models but also plays a crucial role in the models designed for ductile materials such as metals, cf. Bažant (1976) or Amstutz et al. (1995), Oliver (1995), Xue and Wierzbicki (2008). In fact, ductile fracture mechanisms under mixed mode I/II load show either shear, or microvoid coalescence behaviors (Maccagno and Knott 1992), with the latter here modeled by the introduction of ζ.

In most metals, ductile fracture is an elasto-plastic process (Nemat-Nasser 2004; Lubliner 1990; Jirásek and Bažant 2002; Xue and Wierzbicki 2008). Plastic effects are classically understood as a state of the body where external loading and/or thermal fluxes have created residual stresses and irreversible deformations of

N. Van Goethem (✉)
Faculdade de Ciências, Departamento de Matemática,
Centro de Matemática e Aplicações Fundamentais,
Universidade de Lisboa, Av. Prof. Gama Pinto 2, 1649-003,
Lisboa, Portugal
e-mail: vangoeth@ptmat.fc.ul.pt

P. Areias
Physics Department, University of Évora,
Colégio Luís António Verney, Rua Romão Ramalho, 59,
7002-554 Évora, Portugal

the metal. As induced and enhanced by mutual interaction of point defects and dislocations, plastic effects are, as damage, particularly observed in a region around the crack tip called the process zone. These effects are localised along the so-called flow tensor $\mathcal{N}$ which is the derivative of the yield function with respect to the Kirchhoff stress tensor. In order to avoid singular points on the yield surface where $\mathcal{N}$ is undefined (thence belonging to a normal cone), multisurface plasticity is here considered (Klisinski 1998; Areias et al. 2012a).

The present model is applied to metal plasticity which is known to produce higher plastic than elastic deformations. Nevertheless, finite strain elasto-plasticity (Rousselier et al. 1989; Bonet and Wood 2008) will be considered with a multiplicative decomposition of the deformation gradient (Lee 1969). Numerical simulations will be performed with the SIMPLAS code (https://ssm7.ae.uiuc.edu:80/simplas) as based on a series previously published contributions (Areias and Rabczuk 2010; Areias et al. 2009, 2011b, 2012a). Triangular finite elements without tip mesh refinement are used with remeshing performed at every iteration to allow crack propagation. Moreover, the flow law is solved directly, i.e., without appealing to return-map algorithms (Simo and Hughes 1998), by smoothing the complementarity conditions (Chen and Mangasarian 1996).

Obviously, dissipation phenomena are observed at the crack tip, and hence any realistic model should incorporate the temperature (T) as a thermodynamic variable, besides the left Cauchy–Green tensor. In the present model, the energy equation (with a heat source depending on the plastic dissipation) is solved as coupled to the momentum equation, while the yield functions also depend on T. A first series of ductile crack propagation results with such a temperature-dependence have been performed and discussed in Van Goethem et al. (2011) from which the present contribution has followed. However as opposed to the present model the crack propagation direction was calculated with an empirical law based on a CTOD[1] criterion (Ma et al. 1999) which is known to provide excellent qualitative results for both brittle and ductile fracture (cf., e.g., Sutton et al. 2000; Areias et al. 2009, 2011b).

Here we propose a model where the direction of crack propagation follows from rational mechanics arguments from Gurtin's theory of configurational forces (Gurtin 2000). The so-called tip traction is calculated as the limit of a contour integral around the crack tip as the contour converges to the tip. For homogeneous elastic bodies, the tip traction is known to be independent of the chosen contour and corresponds to the notion of J-integral (Sosa and Eischen 1986). However Gurtin's concepts are formulated in such a way that extension to finite strain elasto-plasticity and incorporation of temperature-dependent laws is easily tractable (Gurtin 1981). Moreover fracture criteria based on the J-integral are known to be geometry-dependent, whereas Gurtin's energy release rate criterion is only material dependent.

Our intention in this paper is to show that such a rational fracture criterion (remark that crack tip velocity is also provided) is able to provide remarkable results for two classical benchmark cases, the mode I and mode II crack propagation. Moreover mixed-mode experimental results as reported by Sutton et al. (2000) have been reproduced by our model with good agreement. To conclude the series of numerical simulations, a force-free crack propagation is also shown as an application of the model. Here fracture is driven by the sole heat flux. Note that as opposed to other approaches as based on configurational forces, no tip refinement is required and the contour integral is computed directly (i.e., is not turned into a surface integral by Green's theorem).

Let us emphasize that the present model is based on the so-called Hill–Mandel principle of maximal dissipation (Mandel 1971). First, the plastic flow law follows from the principle of maximal plastic dissipation (Simo 1988a,b; Doghri 2000). In addition, the kinking angle is also a consequence of this principle as applied to crack tip dissipation with appropriate constitutive relations (Gurtin 2000). Let us also remark that as based on this principle it is also possible to theoretically justify crack nucleation criteria for brittle fracture (Van Goethem and Novotny 2010) whereas nucleation of ductile bodies is to the knowledge of the authors not addressed much in the literature from a theoretical viewpoint. We also leave numerical experiences of crack nucleation with this model for future works, and hence the shown examples here are all given with an initial notch. To conclude, let us recall that for ductile fracture the crack tip singularities are less severe than for brittle cracks, and hence the difficulty to deal with in the present model are rather towards the complexity of the global system to solve numerically, which is both nonlinear and non smooth.

[1] Crack Tip Opening Displacement.

2 The fracture model

2.1 On the concept of configurational force

Gurtin (2000) believes that besides the Newtonian force system, the "configurational forces should be viewed as basic objects consistent with their own force balance". Since a body is free to move in its current configuration by the action of the Newtonian forces, whereas it is not free to move in its reference configuration, Gurtin justifies the existence of internal, *material forces* as those that "pin, in place, the material points of the body, thereby maintaining its internal structure".

These notions are rather abstract, requiring to take some distance from our intuition about forces, while conferring to the force the status of a mathematical concept. Moreover, the balance laws of configurational forces follow from rational thermodynamic arguments such as invariance with respect to change in the *material* observer as the exact analogue of Newtonian laws as derived from invariance principles with respect to change in the *spatial* observer. Moreover Gurtin introduces the counterpart of a control volume in the current configuration, called the *material control volume* $P(t)$ that migrates through the reference body and invokes a nonclassical version of the second law requiring that

$$\frac{d}{dt}\{\texttt{free energy of } P(t)\} \leq \{\texttt{rate at which work is performed in } P(t)\}.$$

In Gurtin (2000), these concepts are also specifically developed to study the propagation of a crack.

Let us give a recent interpretation of configurational forces by Gupta and Markenscoff (2008), which is illuminating, since it states the *equivalence* between the classical balance laws (i.e., of Newtonian forces) and the work done by the configurational forces: the aforementioned authors prove that the energy release (associated with the configurational force) "ensures that the body remains infinitesimally close to equilibrium even after a small perturbation of the inhomogeneity position." A further refinement of their approach can be found in Li and Gupta (2006), Gupta and Markenscoff (2007).

2.2 Preliminary results for the model

Let us assume the multiplicative decomposition of the deformation gradient $\mathbf{F}$, i.e., the existence of a local plastic process associated to a local reference configuration and a plastic deformation $\mathbf{F^p}$ such that

$$\mathbf{F} = \mathbf{F^e}\mathbf{F^p}, \tag{2.1}$$

where $\mathbf{F^e}$ defines the elastic deformation (Lee 1969; Truesdell and Noll 2004).

Definition 1 The free energy is a function $\hat{\Psi}$ of the left Cauchy–Green tensor $\mathbf{b^e} := \mathbf{F^e}\mathbf{F^{e}}^T$ and of the temperature T:

$$\begin{aligned}\Psi(X,t) &= \tilde{\Psi}(\mathbf{F}(X,t), \mathbf{F^p}(X,t), T(X,t);\\ \zeta(X,t)) &= \hat{\Psi}(\mathbf{b^e}(X,t), T(X,t)),\end{aligned} \tag{2.2}$$

with an implicit dependence on the auxiliary (scalar, internal) variable ζ which represents damage.

Note that the free energy does not depend explicitly on the damage coefficient, but $\mathbf{b^e}$ depends on ζ through the yield function dependence on ζ and the flow rules (cf. Sect. 3.2 for detail). Let us remark that the material inhomogeneity is due to temperature-dependence of the free energy but also provoked by the assumed non-vanishing plastic deformations $\mathbf{F^p}$, in such a way that $\mathbf{b^e} \neq \mathbf{F}\mathbf{F}^T$.

Let Ω denote the reference body and $[0, t^\star]$ be the interval of time where the evolution of a crack will be considered. We intend to analyze and perform numerical simulations of ductile fracture, a representation of which is shown in Fig. 1.

Let t be the current time and $\boldsymbol{Z}(t) \in \Omega$ denote the crack tip. Moreover, following Gurtin (2000) $D_\delta(t)$ designates the disk centered at $\boldsymbol{Z}$ and of radius $\delta > 0$, $P(t)$ is a so-called "tip control volume", and $P_\delta(t) = P(t) \setminus D_\delta(t)$ is a family of bulk control volumes converging to P.

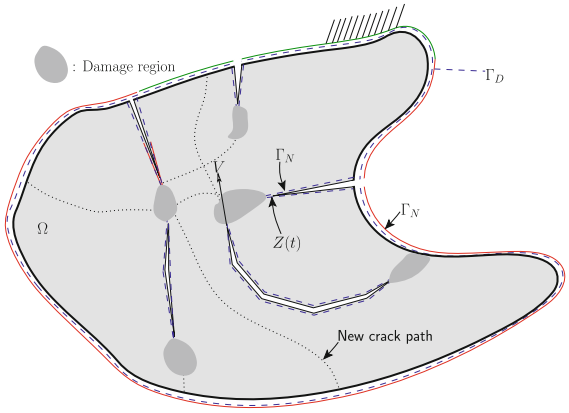

Fig. 1 Ductile fracture in the deformed configuration

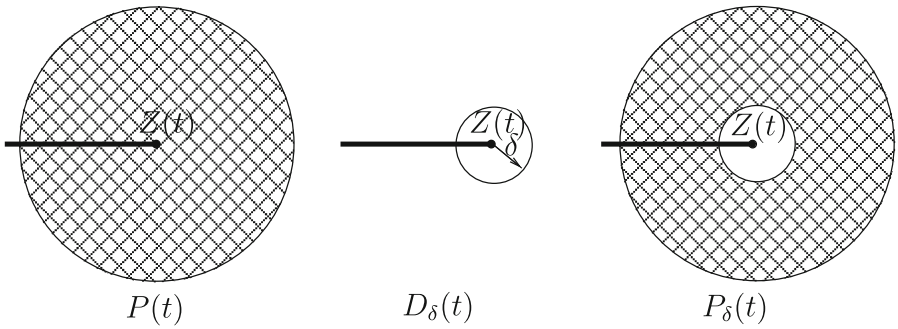

Fig. 2 The notions of crack control volume P, the crack tip disk D_δ and the definition of P_δ

Definition 2 (*Tip integrals*) Recalling Fig. 2, the following tip integrals are defined

$$\oint_{tip} h dL = \lim_{\delta\to 0} \oint_{\partial D_\delta} h dL \quad \text{and} \quad \int_{tip} H dS = \lim_{\delta\to 0} \int_{D_\delta} H dS,$$

where the functions h and H have appropriate regularity.

Definition 3 (*Time derivative following* ∂P) Let $\boldsymbol{q}$ be a velocity field for the particle labeled by $\boldsymbol{X} \in \partial P(t)$. Its trajectory $\boldsymbol{\chi}(\tau)(t \le \tau \le t^\star)$ is defined as the solution of $\dot{\boldsymbol{\chi}}(\tau) = \boldsymbol{q}(\boldsymbol{\chi}(\tau), \tau)$ with $\boldsymbol{\chi}(t) = \boldsymbol{X}$. The time derivative of a field Ψ following ∂P is defined as

$$\overset{\circ}{\Psi}(\boldsymbol{X}, t) := \frac{d}{d\tau}\Psi(\boldsymbol{\chi}(\tau), \tau)_{|\tau=t}. \tag{2.3}$$

Since they serve as basis of our model, we here recall the three following assumption, lemma and definition which are also proved and discussed in Gurtin (2000).

Assumption 1 (*Regular free energy*) Let us assume that the free energy Ψ is smooth away from the tip and that its integral and the integral of its material derivative over P exist in terms of their Cauchy principal value, i.e.,

$$\int_P \Psi dS := \lim_{\delta\to 0} \int_{P_\delta} \Psi dS < \infty$$
$$\text{and} \quad \int_P \overset{\circ}{\Psi}\, dS := \lim_{\delta\to 0} \int_{P_\delta} \overset{\circ}{\Psi}\, dS < \infty. \tag{2.4}$$

Lemma 1 *Under Assumption 1, it holds, uniformly in time:*

$$\lim_{\delta\to 0} \int_{D_\delta} \Psi dS = 0 \quad \textit{and} \quad \lim_{\delta\to 0} \frac{d}{dt} \int_{D_\delta} \Psi dS = 0. \tag{2.5}$$

Remark 1 In the above lemma, the integral $\int_{D_\delta} \Psi dS$ should be understood "in principal part", that is, as defined by (2.4)a. Moreover, if Ψ and $\overset{\circ}{\Psi}$ are assumed norm-integrable in Ω (i.e., $\Psi, \overset{\circ}{\Psi} \in L^1(\Omega)$) then obviously Assumption 1 and Lemma 1 will hold with $\int_{D_\delta} \Psi dS$ indented in the L^1 sense.

Let $\mathbf{N}$ be the exterior unit normal to $\partial D_\delta(t)$ and $\mathbf{T}$ be the crack direction at time t.

Definition 4 By Lemma 1 and in the absence of bulk forces and surface tension on the crack, the dissipation at the crack tip is defined as

$$\Gamma_{tip} := \oint_{tip} (\mathbf{PN} \cdot \dot{\mathbf{y}} + V\mathbf{N} \cdot \mathbf{T}\Psi) dL, \tag{2.6}$$

where $\mathbf{y}(\boldsymbol{X})$ is the position of material point $\boldsymbol{X}$ in the deformed configuration and $\dot{\mathbf{y}}(X, t)$ the motion velocity of $\boldsymbol{X}$. Moreover, V is the crack tip speed, $\mathbf{P}$ the first Piola–Kirchhoff stress[2], and $\mathbf{N}$ the external unit normal to the contour.

2.3 Configurational forces with finite elastoplastic strains

In contrast with Gurtin, we do not require that the internal configurational force $\mathbf{g}$ be integrable in the sense of Cauchy (cf. Assumption 1). In fact be believe that this condition is too restrictive and in particular does not allow for explicit concentration properties at the crack tip. We believe that the notion of Radon measure is much more appropriate in view of the Radon–Nykodým (or Lebesgue) decomposition (cf., e.g., Mattila 1995) of such a measure in a diffuse regular part which is $L^1(\Omega)$ and in a singular part which we here

[2] Identified with the Cauchy stress for small strains.

assume to be purely concentrated. Moreover, a measure is by definition an *extensive* field, and this property is required to confer to $\mathbf{g}$ the interpretation of a force: both the regular integrable and the concentrated parts are extensive fields, whereby all non-measure concentrated distributions are excluded as tip forces.

Assumption 2 The internal body force $\mathbf{g}$ is assumed to be finite Radon measure on Ω, whose singular part is purely concentrated at $\boldsymbol{Z}$, that is, by Radon–Nykodým decomposition,

$$\mathbf{g} = \tilde{\mathbf{g}} + \mathbf{g}^{\star}\delta_{\boldsymbol{Z}} \tag{2.7}$$

with $\tilde{\mathbf{g}}$ Lebesgue-integrable on Ω.

Remark 2 It should however be precised that for the purpose of the present work, $\mathbf{g}$ could have been chosen Lebesgue-integrable only, i.e., without allowing for a concentrated body force contribution. The choice of assuming $\mathbf{g}$ as a measure is made because, on the one hand, it does not render the forthcoming exposition more complicated, and on the other hand because from a physical viewpoint, there exists situations where concentrated forces must be accounted for, as for instance as soon as dislocations are present.

Assumption 3 Let us assume that tensor $\mathbf{C} := \Psi I - \mathbf{F}^T\mathbf{P}$ belongs to $\mathcal{C}(\Omega\backslash\{\boldsymbol{Z}\};\mathbb{R}^{3\times 3})$ and satisfies $\mathrm{Div}\,\mathbf{C} \in \mathcal{M}(\Omega;\mathbb{R}^{3\times 3})$.

The following result is a straightforward extension of a result by Gurtin (2000).

Lemma 2 (Balance laws) *For any tip control volume D, the standard and configurational force balances and the second Law entail that* [3]

$$\int_{\partial D} \mathbf{P}\mathbf{N}\, dL = 0 \tag{2.8}$$

$$\int_{\partial D} (\Psi\mathbf{I} - \mathbf{F}^T\mathbf{P})\mathbf{N}\, dL + \int_{D} \mathbf{g}\, dS + \mathbf{g}_{tip} = 0, \tag{2.9}$$

where $\mathbf{g}_{tip}$ is Gurtin's internal configurational force. Then,

$$\begin{aligned} &\mathrm{Div}\,\mathbf{P} = 0 \quad \textit{and} \quad \mathbf{g} + \mathrm{Div}\,\mathbf{C} = -\mathbf{g}_{tip}\delta_{\boldsymbol{Z}} \\ &\qquad \textit{with} \quad \mathbf{C} := \Psi I - \mathbf{F}^T\mathbf{P}, \end{aligned} \tag{2.10}$$

and where Div *is a symbol recalling the distributional nature of the divergence.*

[3] We write $\mathcal{G} := \int_D \mathbf{g} dS$ with an abuse of notations. It should be written $\mathcal{G} = \int_D \tilde{\mathbf{g}} dS + \mathbf{g}^{\star}(\mathbf{Z})$.

Note that in component form $\mathbf{g} + \mathbf{g}_{tip}\delta_{\boldsymbol{Z}} = -\mathrm{Div}\,\mathbf{C}$ writes by (2.8) and (2.10) as

$$\begin{aligned} \tilde{g}_i + (g^{\star} + g_{tip})_i\delta_{\boldsymbol{Z}} &= -D_j C_{ij} = -D_j(\Psi\delta_{ij} - F_{ki}P_{kj}) \\ &= -D_i\Psi + D_j(F_{ki}P_{kj}) \\ &= s\partial_i T - \Sigma^e_{kl} D_i b^e_{kl} + P_{kj} D_j F_{ki}, \end{aligned} \tag{2.11}$$

where D_i denotes the distributional derivative, and where we have defined the *plastic thermodynamic stress* and the *entropy* as[4]

$$\text{PLASTIC THERMODYNAMIC STRESS:}\quad \Sigma^{\mathbf{e}} := \frac{\partial\hat{\Psi}}{\partial\mathbf{b}^{\mathbf{e}}} = \frac{1}{2}\mathbf{P}\mathbf{F}^T\mathbf{b}^{\mathbf{e}-1} \tag{2.12}$$

$$\text{ENTROPY:}\quad s := -\frac{\partial\hat{\Psi}}{\partial T}. \tag{2.13}$$

In view of Eqs. (2.4) and (2.5) it is still assumed that (cf. Assumption 1 with P here taken as D_δ),

$$\lim_{\delta\to 0}\int_{D_\delta} s\nabla T\, dS = 0. \tag{2.14}$$

By (2.8)–(2.14) and recalling the definition of D_δ on Fig. 2, it results that $\forall\delta > 0$,

$$(\mathbf{g}^{\star} + \mathbf{g}_{tip})\delta_{\boldsymbol{Z}} := -\lim_{\delta\to 0}\int_{D_\delta} \mathrm{Div}\,\mathbf{C}\, dS \tag{2.15}$$

Let us rewrite Eq. (2.9) with D replaced by D_δ, and let $\delta \to 0$. Then by Lemma 1, it also holds

$$(\mathbf{g}^{\star} + \mathbf{g}_{tip})\delta_{\boldsymbol{Z}} = -\lim_{\delta\to 0}\int_{\partial D_\delta} \mathbf{C}\mathbf{N}\, dL, \tag{2.16}$$

for every $\delta > 0$.

As a consequence, recalling (2.11), Definition 2 and Lemma 1, and letting $\delta \to 0$, the crack tip tractions are introduced as follows.

Definition 5 (*Crack tip tractions*)

$$\mathbf{j} := \oint_{tip} (\Psi\mathbf{I} - \mathbf{F}^T\mathbf{P})\mathbf{N}\, dL \tag{2.17}$$

$$\mathbf{i} := \frac{\mathbf{j}}{\|\mathbf{j}\|}. \tag{2.18}$$

[4] To establish (2.12) we have used $\boldsymbol{\tau} = \mathbf{P}\mathbf{F}^T$ together with $\boldsymbol{\tau} = \boldsymbol{\tau}(\mathbf{b}^{\mathbf{e}}, T) := 2\frac{\partial\Psi}{\partial\mathbf{b}^{\mathbf{e}}}\mathbf{b}^{\mathbf{e}}$.

Let us now introduce the classical definition of energy release rate, which will suffice for the application purposes of the present work.

Definition 6 (*Energy release rate*)

$$f := \mathbf{j} \cdot \mathbf{T}, \tag{2.19}$$

where the unit vector $\mathbf{T}$ being the crack direction.

The following Lemma can also be found in Gurtin (2000).

Lemma 3 (Dissipation) *The second law and the balance of configurational forces entail*

$$\Gamma_{tip} = fV \geq 0 \quad with \quad V, f \geq 0. \tag{2.20}$$

Corollary 1 (Crack tip speed) *It follows from* (2.6) *and* (2.20) *that*

$$V = \left\langle \frac{P^*_{tip}}{f^*} \right\rangle_+ \tag{2.21}$$

with $P^*_{tip} := \oint_{tip} (\mathbf{PN}) \cdot \dot{\mathbf{y}} dL$ *and* $f^* := -\oint_{tip} (\mathbf{F}^T\mathbf{P}) \cdot (\mathbf{T} \otimes \mathbf{N}) dL$, *while* $\langle \cdot \rangle_+$ *denotes the "positive part" function defined as* $\langle x \rangle_+ = \frac{x+|x|}{2}$.

Proof From (2.6), (2.19) and (2.20),

$$V \oint_{tip} (\Psi \mathbf{I} - \mathbf{F}^T\mathbf{P})\mathbf{N} dL \cdot \mathbf{T} = \oint_{tip} (\mathbf{PN}) \cdot \dot{\mathbf{y}} dL + V \oint_{tip} (\Psi \mathbf{I}) \cdot (\mathbf{N} \otimes \mathbf{T}) dL,$$

from which (2.21) follows with the positive part $\langle \cdot \rangle_+$ taken because V is assumed nonnegative. □

2.4 Dissipation at the crack tip and kinking

The following statement is taken from Gurtin (2000).

Assumption 4 (*Constitutive assumptions*) Let θ be the kinking angle at time t, i.e. the crack is assumed to propagate in a direction forming a counter-clockwise angle θ with $\mathbf{T}$, i.e. $\mathbf{T} = \hat{\mathbf{T}}(\theta)$, with $\boldsymbol{n} = \mathbf{T}' = \hat{\boldsymbol{n}}(\theta)$, the normal to the crack. It is assumed that

$$f = \hat{f}(\theta) = \mathbf{j} \cdot \hat{\mathbf{T}}(\theta), \tag{2.22}$$

with $\mathbf{j}$ as defined by (2.17) independent of θ. Moreover, the tip speed V is assumed isotropic, i.e., $V = \hat{V}(f)$, and satisfying

$$V, V', V'' > 0 \quad \text{if} \quad f \geq f_{crit} > 0. \tag{2.23}$$

Then, Eq. (2.20) and Assumption 4 yield $\Gamma_{tip}(\theta) = f(\theta)\hat{V}(\hat{f}(\theta))$ with

$$\Gamma'_{tip}(\theta) = (f)'(V'f + V) \quad \text{and}$$
$$\Gamma''_{tip}(\theta) = (f)''(V'f + V) + ((f)')^2(V''f + 2V') \tag{2.24}$$

where, by (2.22),

$$(f)' = \mathbf{j} \cdot \hat{\mathbf{N}}(\theta) \quad \text{and} \quad (f)'' = -f. \tag{2.25}$$

In classical fracture mechanics, the principle of maximal dissipation is often postulated (Mandel 1971). It is also our approach to follow Gurtin with this respect, thereby assuming this principle, whose major consequence is to determine the crack propagation direction $\hat{\mathbf{T}}(\theta^{\text{MAX}})$ as aligned with $\mathbf{j}$.

Law 1 (Maximal dissipation) *The internal variables at time t are such that the dissipation* Γ_{tip} *is maximized at the crack tip.*

Theorem 1 (Crack propagation direction) *Assume that the crack kinks at time t along a direction* $\hat{\mathbf{T}}$ *forming a counter-clockwise angle* θ^{MAX} *with its orientation at time t in order to maximize the dissipation* Γ_{tip} *at* θ^{MAX}. *Then, recalling* $\mathbf{j}$ *as given by* (2.17), *one has*

$$\mathbf{i} = \frac{\mathbf{j}}{\|\mathbf{j}\|} = \hat{\mathbf{T}}(\theta^{\text{MAX}}). \tag{2.26}$$

Proof From (2.24), the critical states of the dissipation are given by

$$\theta \in \Theta^e := \{(f)' = 0\} \quad \text{if} \quad V' \geq 0. \tag{2.27}$$

Moreover at critical points the dissipation is maximized, since

$$\Gamma''_{tip}(\Theta^e) = -f(V'f + V) < 0. \tag{2.28}$$

As a consequence, the kinking angle maximizing the tip dissipation is $\theta^{\text{MAX}} \in \Theta^e$ such that $(f)'(\theta^{\text{MAX}}) = \mathbf{j} \cdot \hat{\boldsymbol{n}}(\theta^{\text{MAX}}) = 0$ from which (2.26) follows. □

2.5 When, where and how much does crack propagate?

- **When?** As soon as the critical void fraction is reached, i.e., $\zeta = \zeta_{\text{crit}}$, cf. the model equations below (see Eq. (3.1)).
- **Where?** In the direction of θ^{MAX}, that is, as parallel to the tip traction cf. Eq. (2.17).
- **How much?** With a velocity V given by (2.21) while the quasistatic time-step δt is fixed.

3 Balance and flow laws

The solution will consist in solving coupled balance and flow lows.

3.1 Temperature-dependent compressible neo-Hookean isotropic finite strain elasticity

The (homogeneous and isotropic)[5] compressible neo-Hookean free energy reads (Doghri 2000)

$$W(\mathbf{F},\mathbf{F}^{\mathbf{p}}) = \tilde{W}(\mathbf{F}\mathbf{F}^{-\mathbf{p}}, I) = \hat{W}(\mathbf{b}^{\mathbf{e}}) := \frac{\mu}{2}\left(J_{\mathrm{e}}^{-2/3}\,\mathrm{tr}\,\mathbf{b}^{\mathbf{e}} - 3\right) + \frac{\kappa}{2}(1-J_{\mathrm{e}})^2, \tag{3.1}$$

with $\mathbf{F}^{-\mathbf{p}} := (\mathbf{F}^{\mathbf{p}})^{-1}$, $\mathbf{b}^{\mathbf{e}} := \mathbf{F}^{\mathbf{e}}\mathbf{F}^{\mathbf{e}T}$ (recall that $\mathbf{F} = \mathbf{F}^{\mathbf{e}}\mathbf{F}^{\mathbf{p}}$) and $J_{\mathrm{e}} := \sqrt{\det \mathbf{b}^{\mathbf{e}}}$. This energy is known to be well-defined for metal plasticity (where elastic strains are smaller than plastic strains).[6]

The associated temperature-dependent free energy (per unit volume) reads

$$\hat{\Psi}\left(\mathbf{b}^{\mathbf{e}}, \bar{\epsilon}_i^p, T\right) := \hat{W}(\mathbf{b}^{\mathbf{e}}) + (3\lambda+2\mu)\tilde{\alpha}(T-T_{\mathrm{env}})(1-J_{\mathrm{e}}) - \frac{C_p\rho}{2T_{\mathrm{env}}}(T-T_{\mathrm{env}})^2 + \mathcal{H}\left(\bar{\epsilon}_i^p\right), \tag{3.2}$$

with $\tilde{\alpha}$ the coefficient of thermal expansion, and where $\mathcal{H}$ is the hardening term with the hardening variables chosen as the equivalent plastic strain $\bar{\epsilon}_i^p$ ($i = 1, 2$), which are with $\mathbf{b}^{\mathbf{e}}$ the problem unknowns, whose solution is given by the flow laws in Sect. 3.2. Here, we consider isotropic hardening with $\mathcal{H}(\bar{\epsilon}_i^p) = \frac{1}{2}\sum_{i=1}^2 H_i(\bar{\epsilon}_i^p)^2$ with $H_i \geq 0$.

Let us also define $\mathbf{l} := \dot{\mathbf{F}}\mathbf{F}^{-1}$, $\mathbf{d} = \frac{1}{2}(\mathbf{l}+\mathbf{l}^T)$ and $\overset{\star}{\mathbf{b}}{}^{\mathbf{e}}$ as the derivative of $\mathbf{b}^{\mathbf{e}}$ while keeping $\mathbf{F}$ constant.[7]

We introduce the *plastic rate of deformation* as (cf. Bonet and Wood 2008; Areias et al. 2012a for detail),

$$\mathbf{l}^{\mathbf{p}} := -\frac{1}{2}\,\overset{\star}{\mathbf{b}}{}^{\mathbf{e}}\,(\mathbf{b}^{\mathbf{e}})^{-1} = \frac{1}{2}\mathbf{F}\mathbf{C}^{-\mathbf{p}}\dot{\mathbf{C}}^{\mathbf{p}}\mathbf{F}^{-1}, \tag{3.3}$$

and the *elastic rate of deformation* as

$$\mathbf{l}^{\mathbf{e}} := \dot{\mathbf{F}}^{\mathbf{e}}\mathbf{F}^{-\mathbf{e}}. \tag{3.4}$$

By Clausius–Duhem inequality, $\boldsymbol{\tau}\cdot\mathbf{d} - \frac{d}{dt}(\hat{W}+\mathcal{H}) \geq 0$ for any process, which we rewrite as (Maugin (1992), Bonet and Wood (2008)) $(\boldsymbol{\tau} - 2\frac{\partial \hat{W}}{\partial \mathbf{b}^{\mathbf{e}}}\mathbf{b}^{\mathbf{e}})\cdot\mathbf{l}^{\mathbf{e}} + \boldsymbol{\tau}\cdot\mathbf{l}^{\mathbf{p}} - \sum_{i=1}^2 q_i^\star\,\dot{\bar{\epsilon}}_i^p \geq 0$ with the hardening stress $q_i^\star := H_i\bar{\epsilon}_i^p$, whereby the Kirchhoff stress is defined as $\boldsymbol{\tau}(\mathbf{b}^{\mathbf{e}}, T) := 2\dfrac{\partial\Psi}{\partial \mathbf{b}^{\mathbf{e}}}\mathbf{b}^{\mathbf{e}}$, that is, in plane stress (note that the factor $E/(1-\nu)$ should be replaced by $(3\lambda+2\mu)$ in plane strain or in $3D$) (Areias et al. 2012a),

$$\boldsymbol{\tau}(\mathbf{b}^{\mathbf{e}}, T) = \mu J_{\mathrm{e}}^{-2/3}\left(\mathbf{b}^{\mathbf{e}} - \frac{\mathrm{tr}\,\mathbf{b}^{\mathbf{e}}}{d}\mathbf{I}\right) - \left(\kappa(1-J_{\mathrm{e}}) + \frac{\tilde{\alpha}E}{1-\nu}(T-T_{\mathrm{env}})\right)J_{\mathrm{e}}\mathbf{I}, \tag{3.5}$$

with $d = 2$ in plane stress and $d = 3$ in plane strain or in $3D$.

Remark that (2.14) is satisfied with $\boldsymbol{\tau}$ as given by (3.5). Moreover, we introduce the rate of mechanical dissipation as the remaining terms in the LHS of Clausius–Duhem inequality, viz.,

$$\mathcal{D}\left(\boldsymbol{\tau}, q_i^\star; \mathbf{l}^{\mathbf{p}}, \dot{\bar{\epsilon}}_i^p\right) := \boldsymbol{\tau}\cdot\mathbf{l}^{\mathbf{p}} - \sum_{i=1}^2 q_i^\star\,\dot{\bar{\epsilon}}_i^p, \tag{3.6}$$

with $\boldsymbol{\tau}\cdot\mathbf{l}^{\mathbf{p}}$ the rate of plastic dissipation.

Let us assume that $\mathbf{b}^{\mathbf{e}} \in L^2(\Omega)$ with $J_{\mathrm{e}} \in L^\infty(\Omega)$. Since $\mathbf{b}^{\mathbf{e}} = \mathbf{F}\mathbf{C}^{-\mathbf{p}}\mathbf{F}^T =: \hat{\mathbf{b}}^{\mathbf{e}}(\mathbf{F}(\mathbf{u}), \mathbf{F}^{\mathbf{p}}) = \tilde{\mathbf{b}}^{\mathbf{e}}(\mathbf{u}, \mathbf{F}^{\mathbf{p}})$ with $\mathbf{C}^{\mathbf{p}} := \mathbf{F}^{\mathbf{p}T}\mathbf{F}^{\mathbf{p}}$ and where $\mathbf{u}$ is the displacement field, the quasi-static momentum balance law in plane stress reads in the weak form: find $\mathbf{u} \in (H^1(\Omega))^3$ such that:

$$\begin{cases} \displaystyle\int_\Omega \boldsymbol{\tau}(\tilde{\mathbf{b}^{\mathbf{e}}}(\mathbf{u}, \mathbf{F}^{\mathbf{p}}), T)\cdot\nabla\hat{\mathbf{u}}\,dS = \int_{\Gamma_N}\mathbf{G}\cdot\hat{\mathbf{u}}\,dL \\ \tau_{33} = 0, \end{cases} \tag{3.7}$$

for every $\hat{\mathbf{u}} \in (H_0^1(\Omega;\mathbb{R}^3))$ and where $\mathbf{G}$ is the applied load on the boundary (no external body forces are here considered).

The weak form of the heat conduction equation reads: find $T \in H^1(\Omega)$ such that:

$$\int_\Omega (\rho C_p\dot{T}\hat{T} + k\nabla T\cdot\nabla\hat{T})dV = \int_\Omega \rho\tilde{\alpha}(\boldsymbol{\tau}\cdot\mathbf{l}^{\mathbf{p}})\hat{T}\,dV, \tag{3.8}$$

[5] Since it does not dependent explicitly on $\boldsymbol{X}$, but only on $\mathbf{b}^{\mathbf{e}}$, and hence is invariant with respect to rotations (Bonet and Wood 2008); moreover, it dependents on the tensorial invariants of $\mathbf{b}^{\mathbf{e}}$ only. The identity $W(\mathbf{F},\mathbf{F}^{\mathbf{p}}) = \tilde{W}(\mathbf{F}\mathbf{F}^{-\mathbf{p}}, I)$ follows from the principle of plastic invariance (Mielke 2003).

[6] Note however that being non polyconvex, there exist no solution in the framework of pure nonlinear elasticity, i.e., for $\mathbf{F}^{\mathbf{e}} = \mathbf{F}$. In Conti and de Lellis (2003) the authors show that there is no existence of solutions for limit cases, but however it should be noted that they consider an energy involving $(\nabla\mathbf{u})^2$, which is different from $\mathbf{F}\mathbf{F}^T$ and thus also from $\mathbf{F}^{\mathbf{e}}\mathbf{F}^{\mathbf{e}T}$.

[7] Since $\overset{\star}{\mathbf{b}}{}^{\mathbf{e}}$ represents the variation of $\mathbf{b}^{\mathbf{e}}$ due to permanent deformations while the total deformation $\mathbf{F}$ is kept unchanged, $\mathbf{l}^{\mathbf{p}}$ vanishes in the case of pure elastic unloading.

for every $\hat{T} \in H_0^1(\Omega)$ and with $\bar{\alpha}$ the Taylor–Quinney coefficient (i.e., giving the proportion of energy converted into heat), and $\mathbf{l^p}$ the plastic strain rate to be defined below. The specific heat supply is given by

$$\dot{Q} = \bar{\alpha}(\boldsymbol{\tau} \cdot \mathbf{l^p}). \tag{3.9}$$

3.2 Principle of maximal plastic dissipation and flow law

Let us introduce the *maximal principal Almansi strain*

$$\epsilon_{\text{eq}} = \arg\max_{\epsilon_i} \left\{ \det\left((\mathbf{I} - \mathbf{b}^{-\mathbf{e}}) - 2\epsilon_i \mathbf{I}\right) = 0 \right\}, \tag{3.10}$$

the *void fraction* (that, is, the damage parameter),

$$0 \leq \zeta = \left(\frac{\epsilon_{\text{eq}}}{\bar{\varepsilon}}\right)^2 \leq 1, \tag{3.11}$$

with $\bar{\varepsilon}$ a constitutive parameter. The m *yield functions* read $(1 \leq i \leq m = 2)$

$$\Phi_i\left(\boldsymbol{\tau}, \sigma_i^{\text{eq}}\right) := \sigma_i^{\text{eq}} - (1-\zeta)\left(1 - \frac{T - T_{\text{env}}}{T_{\text{melt}} - T_{\text{env}}}\right)\sigma_{yi}, \tag{3.12}$$

with T_{env} and T_{melt} the room and melting temperatures, respectively, with the *yield stress* given by

$$\sigma_{yi} = \sigma_{\text{y}}^0 + H\bar{\epsilon}_i^p, \tag{3.13}$$

with σ_{y}^0 the initial tensile yield stress, with the ith *equivalent plastic strain*

$$\bar{\epsilon}_i^p = \int_0^t \dot{\bar{\epsilon}}_i^p \, ds, \tag{3.14}$$

and H a material-hardening constitutive parameter and where the von Mises and Drucker–Prager *equivalent stresses* read (with $\boldsymbol{\tau}^d$ the deviatoric part of $\boldsymbol{\tau}$)

$$\begin{cases} \sigma_1^{\text{eq}} := \sqrt{\frac{3}{2}\boldsymbol{\tau}^2 - \frac{9}{2d^2}(\operatorname{tr}\boldsymbol{\tau})^2} = \sqrt{\frac{3}{2}(\boldsymbol{\tau}^d)^2} \\ \sigma_2^{\text{eq}} := \qquad\qquad \sigma_1^{\text{eq}} - \beta\zeta \operatorname{tr}\boldsymbol{\tau}. \end{cases} \tag{3.15}$$

with β a constitutive parameter. Here $d = 2$ in plane stress and $d = 3$ in plane strain or in $3D$.
Consider the rate of *mechanical dissipation* $\mathcal{D}(\boldsymbol{\tau}, q_i^\star; \mathbf{l^p}, \dot{\bar{\epsilon}}_i^p)$ as given by (3.6), where $q_i^\star := H\bar{\epsilon}_i^p$.

Theorem 2 (Maximal plastic dissipation) *The principle of maximal plastic dissipation entails the flow laws*[8]

$$\begin{cases} \frac{1}{2}(\mathbf{l^p} + \mathbf{l^{pT}}) = \sum_{i=1}^2 \dot{\lambda}_i \frac{\partial \Phi_i}{\partial \boldsymbol{T}}(\boldsymbol{\tau}, q_i^\star) \\ \qquad\qquad = \sum_{i=1}^2 \dot{\lambda}_i \bar{\boldsymbol{\tau}}(1 - d\beta\zeta\delta_{i2}) \\ \dot{\bar{\epsilon}}_i^p = -\dot{\lambda}_i \frac{\partial \Phi_i}{\partial q_i}(\boldsymbol{\tau}, q_i^\star) \\ \qquad\qquad = \dot{\lambda}_i(1-\zeta)(1 - \frac{T - T_{\text{env}}}{T_{\text{melt}} - T_{\text{env}}}) \end{cases} \tag{3.16}$$

and $c\dot{\lambda}_i - \langle c\dot{\lambda}_i + \Phi_i(\boldsymbol{\tau}, q_i^\star)\rangle_+ = 0$, *where the yield functions are given by (3.12) and* $\bar{\boldsymbol{\tau}} := \frac{\boldsymbol{\tau}^d}{\sqrt{\frac{2}{3}(\boldsymbol{\tau}^d)^2}}$.

Proof The elasticity domain is defined as the convex set $\Xi := \{(\mathbf{T}, q_i) \in \mathcal{A} \text{ s.t. } \phi^\star(\mathbf{T}, q_i) \leq 0\}$ where $\mathbf{T}$ is a symmetric second-order matrix and q_i $(i = 1, 2)$ a scalar. Hill–Mandel's principle of maximal dissipation states that the solution $(\boldsymbol{\tau}, \sigma_i^{\text{eq}})(i = 1, 2)$ satisfies

$$\mathcal{D}\left(\boldsymbol{\tau}, \sigma_i^{\text{eq}}; \mathbf{l^p}, \dot{\bar{\epsilon}}^p\right) = \max_{(\mathbf{T}, q_i) \in \Xi} \left\{ \mathcal{D}\left(\mathbf{T}, q_i; \mathbf{l^p}, \dot{\bar{\epsilon}}^p\right) \right\}. \tag{3.17}$$

From the constraint $\Phi_1 \leq 0$ and $\Phi_2 \leq 0$, the flow rules immediately follow from the stationary points of the Lagrangean $\mathcal{L}(\mathbf{T}, q_i, \dot{\lambda}_i; \mathbf{l^p}, \dot{\bar{\epsilon}}^p) := -\mathcal{D}(\mathbf{T}, q_i; \mathbf{l^p}, \dot{\bar{\epsilon}}^p) + \sum_{i=1}^2 \dot{\lambda}_i \Phi_i(\mathbf{T}, q_i)$ w.r.t $(\mathbf{T}, q_i, \dot{\lambda})$ with the Lagrange multipliers $\dot{\lambda}_i$ and recalling definition (3.6). The last equalities in the RHS of (3.16) follow by the definition of Φ_i. □

From (3.15) & (3.16) and since $\boldsymbol{\tau} \cdot \bar{\boldsymbol{\tau}} = \sigma_1^{\text{eq}}$ while $\Phi_i \dot{\lambda}_i = 0$, the rate of dissipation reads

$$\mathcal{D} = (1-\zeta)\left(1 - \frac{T - T_{\text{env}}}{T_{\text{melt}} - T_{\text{env}}}\right) \sum_{i=1}^2 \dot{\lambda}_i \left(\sigma_{yi}(1 - d\beta\zeta\delta_{i2}) - H\bar{\epsilon}_i^p\right).$$

Let us remark that Eq. (3.16c) is solved directly by means of Chen–Mangasarian function (Chen and Mangasarian 1996). Moreover $\frac{\partial \Phi^\star}{\partial \boldsymbol{\tau}}$ is computed in an exact manner with Mathematica (Wolfram Research Inc. 2007). For a detailed description of the numerical

[8] Noting in passing that the extremization principles has left $\frac{1}{2}(\mathbf{l^p} - \mathbf{l^{pT}})$ undefined, a fact that is not mentioned clear in classical literature. Let us also remark that the set of inequalities for the plastic multiplier and the yield function is given by the formal Eq. (3.16)c where c is a parameter to satisfy unit consistency.

implementation of the model, of computational issues such as mesh opening, remeshing, type of finite elements used we refer to Areias and Rabczuk (2010), Areias et al. (2011b, 2012a,b). Some detail is given in Sect. 4.2.

4 Numerical implementation

4.1 Brief discussion on the numerical method

Combination of the return-mapping technique (Nemat-Nasser 2004; Simo and Hughes 1998) and mixed formulations (Brezzi and Fortin 1991) led to a standardization of elasto-plastic modeling with finite elements (see the treatise by Belytschko et al. 2000 and the one by Bonet 2008). However, return-mapping algorithms where implicit inequality for the plastic multiplier appear still pose challenges to systematization, since the predictor in the presence of ductile damage evolution can give a false indication and might produce fictitious unloading. As a consequence, classical finite strain constitutive approaches (e.g. the rotated $\mathbf{F^e F^p}$ method Areias and Belytschko 2006) inherit some of the difficulties of the small strain algorithms.

Besides these problems, in complex simulations the convergence radius is often not satisfactory (Crisfield and Norris 1999). For ductile fracture problems, where mesh adaptation, quadrature point alterations and even full remeshing has to be adopted, small convergence radius can be impairing for a successful analysis.

Here, the finite strain elasto-plastic algorithm of Areias et al. (2012a) has been adopted, which allows us to include in the same underlying framework, kinematic hardening, anisotropy and damage. Adding to this, recent ductile damage models (specifically the one by Areias et al. 2011a) make use of non-differentiable convex yield functions, not easily tractable by classical return-mapping algorithms.

4.2 Iteration of the historical variables

The time interval $[0, t^\star]$ is discretized and the unknowns are computed at time $t^n \in [0, t^\star]$ with $1 \leq n \leq N$.

To find $\mathbf{F}$ and T at each time iteration, we need to determine the tangent modulus associated to (3.7) and (3.8),

$$\begin{bmatrix} \frac{\partial \dot{Q}}{\partial T} & \frac{\partial \dot{Q}}{\partial \mathbf{F}} \\ \frac{\partial \boldsymbol{\tau}}{\partial T} & \frac{\partial \boldsymbol{\tau}}{\partial \mathbf{F}} \end{bmatrix},$$

which is computed with Mathematica and the AceGen add-on Korelc (2002).

Then, having solved (3.7) at time t_{n+1} knowing the solution at time t_n, the increment of $\mathbf{F}$ is found as

$$\delta \mathbf{F_n} = \mathbf{F_{n+1}} \mathbf{F_n}^{-1}$$

From the expression $\mathbf{b^e} = \mathbf{F C^{-p} F}^T$ we infer that $\mathbf{b^e}$ at time t_{n+1} writes as

$$\begin{aligned} \mathbf{b^e_{n+1}} &= \mathbf{F_{n+1}} \mathbf{C^{-p}}_n \mathbf{F_{n+1}}^T \\ &+ \delta \overset{\star}{\mathbf{b}}{}^{\mathbf{e}}_{\mathbf{n}} = \mathbf{F_{n+1}} \left(\mathbf{F_n}^{-1} \mathbf{b^e_n} \mathbf{F_n}^{-T} \right) \mathbf{F_{n+1}}^T \\ &+ \delta \overset{\star}{\mathbf{b}}{}^{\mathbf{e}}_{\mathbf{n}} = \delta \mathbf{F_n} \mathbf{b^e_n} \delta \mathbf{F_n}^T + \delta \overset{\star}{\mathbf{b}}{}^{\mathbf{e}}_{\mathbf{n}} \end{aligned}$$

where $\delta^\star \mathbf{b^e}$ is the increment of $\mathbf{b^e}$ caused by a variation of $\mathbf{C^p}$. In brief we write

$$\mathbf{b^e_{n+1}} = \mathbf{b}^{\mathbf{e}^\circ}_{\mathbf{n}} + \delta \overset{\star}{\mathbf{b}}{}^{\mathbf{e}}_{\mathbf{n}} \tag{4.1}$$

where $\mathbf{b}^{\mathbf{e}^\circ}_{\mathbf{n}}$ is the "trial" $\mathbf{b^e}$ at time t^n. Then $\boldsymbol{\tau_n} := \boldsymbol{\tau}(\mathbf{b^e_n}, T_n)$ is replaced by $\boldsymbol{\tau_{n+1}}$ and (3.7) is solved iteratively as coupled with the heat equation.

On the other hand $\mathbf{d^p} := (\mathbf{l^p})^S = -\frac{1}{4} \overset{\star}{\mathbf{b}}{}^{\mathbf{e}} \mathbf{b^{-e}} - \frac{1}{4} \mathbf{b^{-e}} \overset{\star}{\mathbf{b}}{}^{\mathbf{e}}$ which as rewritten in Voigt form allows us to isolate $\overset{\star}{\mathbf{b}}{}^{\mathbf{e}}$, that is,

$$\mathbf{d^p_V} = -\frac{1}{4} \boldsymbol{A_V} \overset{\star}{\mathbf{b}}{}^{\mathbf{e}}_{\mathbf{V}} \tag{4.2}$$

where in $3D$, $\boldsymbol{A_V}$ is a 6×6 matrix whose entries are linear combinations of the entries of $(\mathbf{b^e})^{-1}$ (Areias et al. 2012a).

As a consequence, the flow law (3.16) is integrated semi-implicitly. In particular, matrix A is kept constant as a function of $\mathbf{b^e_n}$ and then the flow law reads as the nonlinear system (Voigt notation is used):

$$\begin{cases} 0 = \mathbf{b}^{\mathbf{e}^\circ}_{\mathbf{n}} - \mathbf{b^e_{n+1}} - 4 \boldsymbol{A}_{\boldsymbol{V}}^{-1} \boldsymbol{n}_n \boldsymbol{\delta \dot{\lambda}} \\ 0 = \quad \bar{\epsilon}^p_n - \bar{\epsilon}^p_{n+1} + \varphi_n \delta \dot{\lambda} \\ 0 = \quad c \boldsymbol{\delta \dot{\lambda}} - \langle c \boldsymbol{\delta \dot{\lambda}} + \boldsymbol{\delta \varphi} \rangle_+ \end{cases}, \tag{4.3}$$

with the flow vector $\boldsymbol{n}_n := (\frac{\partial \Phi_1}{\partial \boldsymbol{\tau}}, \frac{\partial \Phi_2}{\partial \boldsymbol{\tau}})(\boldsymbol{\tau_{n+1}}, q_{i\,n+1}; \zeta_n, T_{n+1})$ and $\varphi_n := (\frac{\partial \Phi_1}{\partial q_1}, \frac{\partial \Phi_2}{\partial q_2})(\boldsymbol{\tau_{n+1}}, q_{i\,n+1}; \zeta_n, T_{n+1})$. Moreover, the notation $\boldsymbol{\delta \dot{\lambda}} = (\delta \gamma_1, \delta \gamma_2)^T, \boldsymbol{\delta \Phi} = (\delta \Phi_1, \delta \dot{\Phi}_2)^T, \boldsymbol{\delta \varphi} = (\delta \varphi_1, \delta \varphi_2)^{\mathbf{T}}$ is employed.

The solution of (4.3) provides the constitutive variables at time t^{n+1},

$$\left\{ \mathbf{b^e_{n+1}}, \boldsymbol{\delta \dot{\lambda}}, \bar{\epsilon}^p_{n+1} \right\}^T.$$

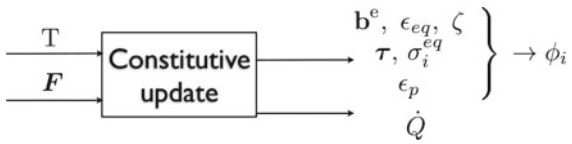

Fig. 3 Summary of the iterative process

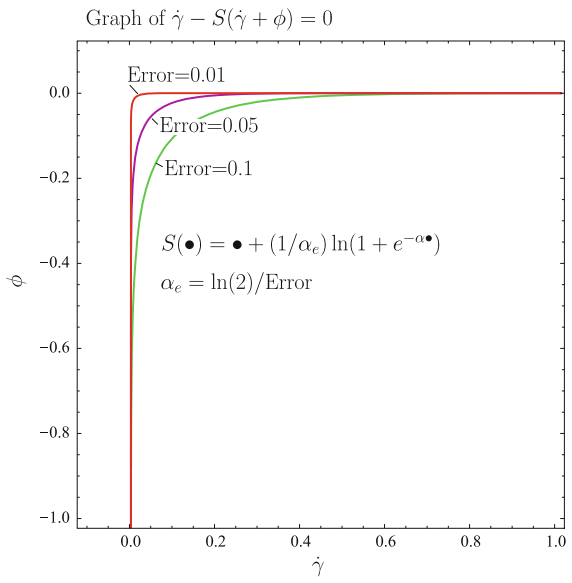

Fig. 4 Approximation of the "positive part" to solve the complementarity conditions (i.e., the flow rules)

A figure summarizing the iterative process is provided in Fig. 3. Supplementary detail on the numerical resolution of (4.3) can be found in Bai and Wierzbicki (2010), Areias et al. (2012a,b).

4.3 Smoothing the complementarity condition

Equation (4.3*c*) is solved be approximating the "positive part" function $\langle\cdot\rangle_+$ by the smooth ramp function (Chen and Mangasarian 1996),

$$\langle x\rangle_+ \sim S(x) = x + \frac{1}{\alpha_e}\ln\left(1 + \exp(-\alpha_e x)\right),$$

as can be observed in Fig. 4.

4.4 Computation of the contour integral and fracture algorithm

The crack tip traction $\mathbf{j}^e$ whose expression is given by (2.17) is computed in the reference configuration as a contour integral on a circle centered at the crack tip and of radius 1/40th of the body diameter.

A picture of the fracture algorithm is provided in Fig. 5.

5 Numerical results

Concerning the algorithm, direct integration of the rate equations is performed as well as smoothing of the complementarity conditions with the Chen–Mangasarian function. The resulting problem is smooth, always converges quadratically and is robust, typically requiring fewer steps than return-mapping algorithms.

Selected examples are shown in the following sections. In the first 2 and last examples no thickness variation was considered. The second example is then re-run with thickness variation (see Sect. 5.3) showing no significant change in the results.

5.1 Ductile fracture in Mode 1 and Mode 2

The fracture model as based on configurational forces is first tested on classical Mode I and Mode II loading experiments. The set-up and the values of the model parameter are shown in Fig. 6. The mode I loading (i.e., pure traction) consists in a imposed displacement perpendicular to the upper and lower faces of the body, while the left-side face is clamped and right-side face is displacement free. For the mode II loading (i.e., pure shear) the imposed displacement is parallel to the upper and lower faces. The left-side face is clamped in its upper half part and force-free in its lower half part, while the right-side face is also force-free. In both cases a notch is inserted in the middle of the left-side face.

Propagation of the crack as loading increases is observed in Figs. 7 (for mode I) and 9 (for mode II) along a path whose direction is given by the principle of maximal dissipation and hence with a kinking angle given by the direction of the tip traction (2.17). The time increment is here 0.1 s. The temperature dependent elasto-plastic problem is solved entirely at each iteration: effective plastic strain, damage and temperature difference (i.e., $T - T_{\text{env}}$) are shown in Figs. 7 and 9, while load-displacement curves are given in Figs. 8 (for mode I) and 10 (for mode II) for 2 mesh refinements, which are shown in Fig. 11.

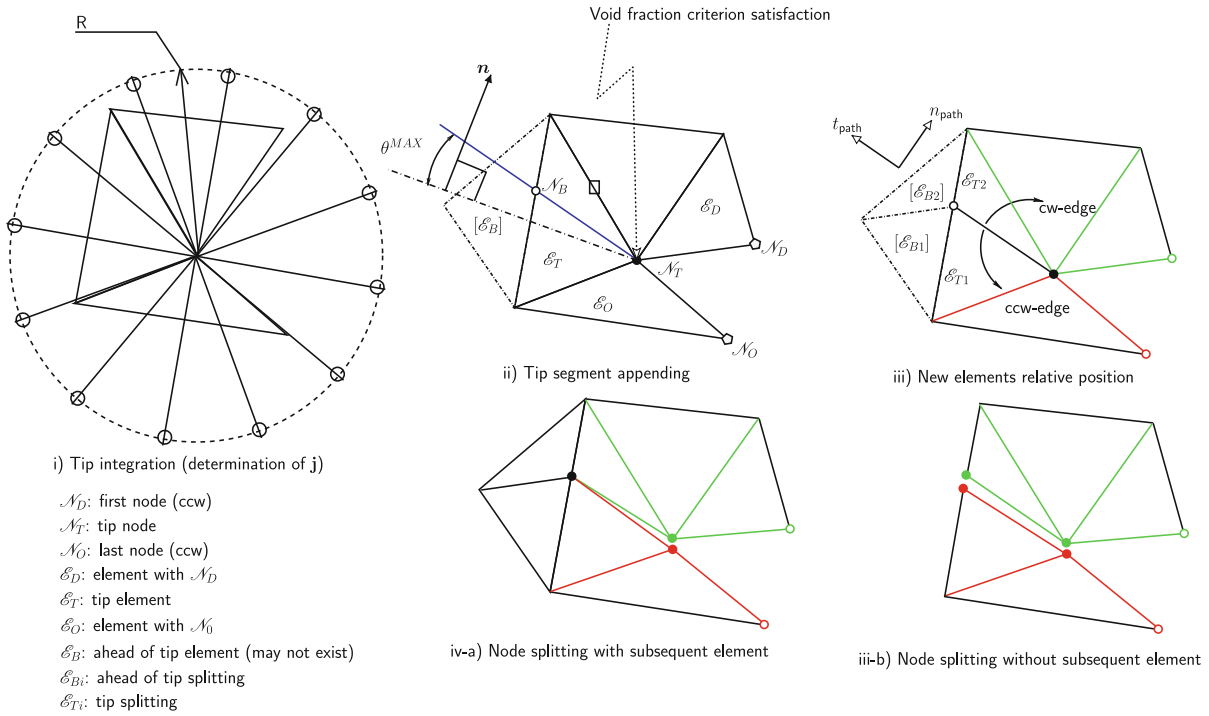

Fig. 5 Fracture algorithm. *Left* the contour integral: the stress is interpolated at 100 points on the circle of radius R; *middle* node splitting and mesh opening; *right*: element re-ordering and splitting

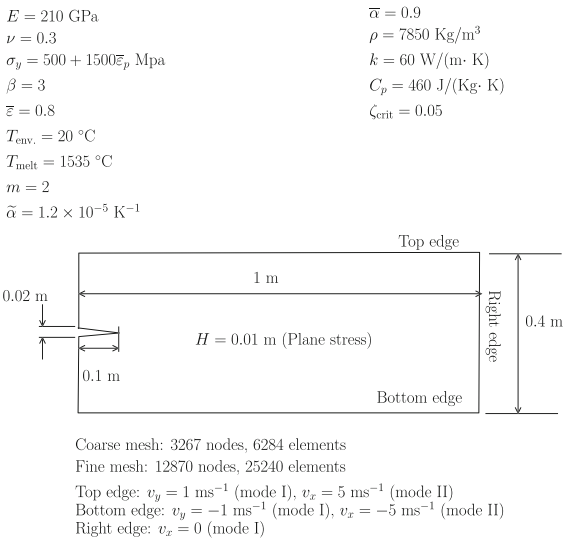

Fig. 6 The set-up and all values of the material and model parameter for the Mode I and Mode II experiments

It is astonishing to observe that the path followed by the Mode I and Mode II cracks are almost identical. In fact, one knows that in brittle fracture the two paths are clearly distinct (cf., e.g., Allaire et al. 2011). However, for ductile fracture this is no more the case as laboratory experiments and numerical simulations show (Maccagno and Knott 1992; Amstutz et al. 1995; James and Swenson 1999; Sutton et al. 2000) (Fig. 12).

From this consideration, it appears mandatory to assess our model with comparison with these known experimental facts. This is done in Sect. 5.2

5.2 The Arcan–Sutton tearing test

The Arcan test fixture as shown in Fig. 13 have been originally used for testing of composite specimens for stable tearing tests (Arcan et al. 1978). We here refer to Sutton et al. (2000) where experimental results by Amstutz et al. (1995) have been reproduced with good qualitative agreement for 2024-T3 aluminum.

Our objective is to assess our criterion based on maximal dissipation and our temperature-dependent finite-strain elasto-plastic model by comparison of the numerically computed crack propagation direction with the known experimental paths for a series of 5 mixed-mode loading angle.

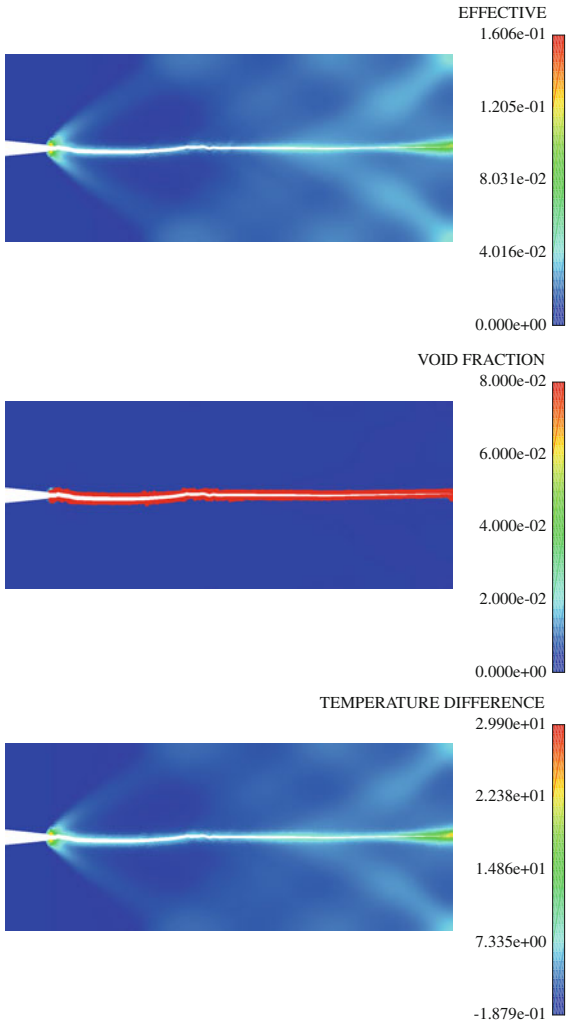

Fig. 7 The effective plastic strain, the damage (i.e., void fraction) parameter and the temperature for the Mode I experiment. The time increment is here 0.1 s

The results shown in Fig. 14 indicate good agreement with the experimental results. The time increment is here 0.1 s. The temperature is also shown along the path in Fig. 14. Therefore it is believed that the proposed model deserves attention towards future applications of ductile fracture.

5.3 ARCAN test with plane stress and thickness variation

Thickness variation is caused by the condition $\tau_{33} = 0$ where 3 is the out-of-plane direction. Since the

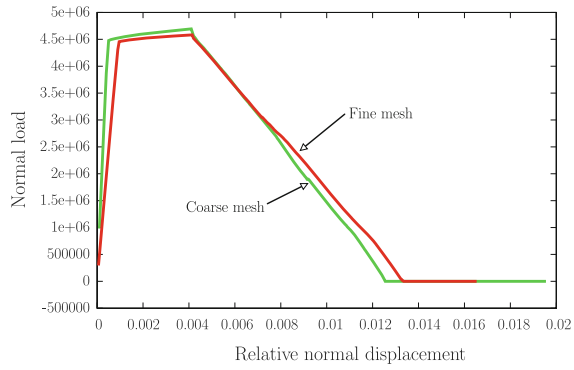

Fig. 8 Displacement-loading curves for coarse and fine meshes for the Mode I experiment. A first stable process is followed by an unstable propagation. Coarse mesh consists of 3,270 nodes and 6,284 elements. Fine mesh consists of 12,870 nodes and 25,240 elements

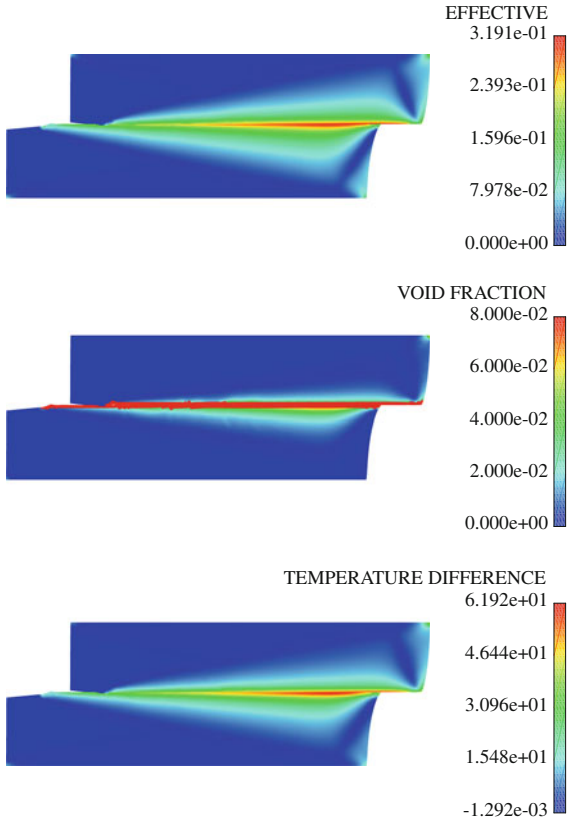

Fig. 9 The effective plastic strain, the damage (i.e., void fraction) parameter and the temperature for the Mode II experiment. The time increment is here 0.1 s

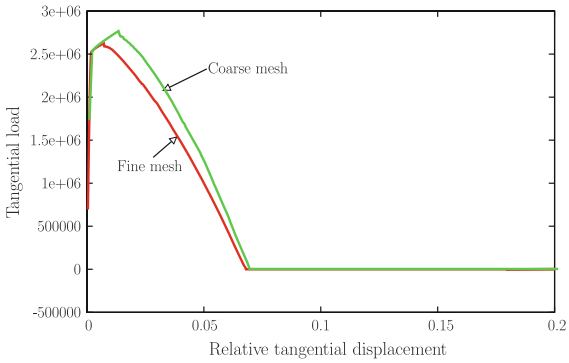

Fig. 10 Displacement-loading curves for coarse and fine meshes for the Mode II experiment. A first stable process is followed by an unstable propagation

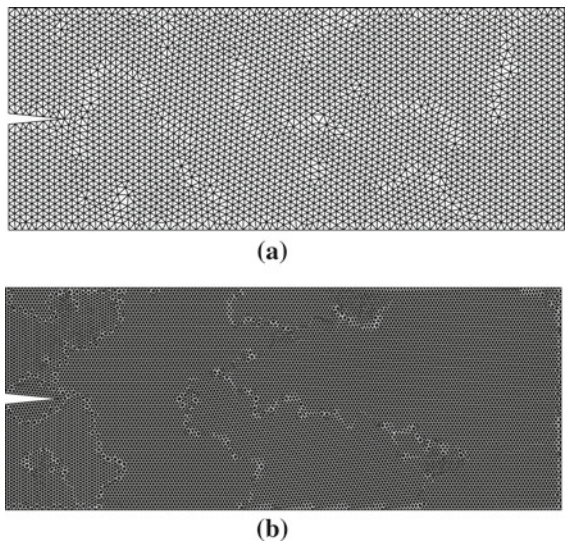

Fig. 11 **a** Coarse mesh consisting of 3,270 nodes and 6,284 elements. **b** Fine mesh consisting of 12,870 nodes and 25,240 elements

deformation gradient for plane stress can be partitioned as

$$\mathbf{F} = \begin{bmatrix} F_{11} & F_{12} & 0 \\ F_{22} & F_{21} & 0 \\ 0 & 0 & F_{33} \end{bmatrix} \tag{5.1}$$

where

$$F_{33} = \frac{h}{H} \tag{5.2}$$

with h and H representing, respectively, the deformed and undeformed thickness, we can therefore impose the condition $\tau_{33} = 0$ by calculating F_{33} and therefore h. The application of Newton's method results as:

$$\frac{\partial \tau_{33}}{\partial F_{33}} \delta F_{33} = -\tau_{33} \tag{5.3}$$

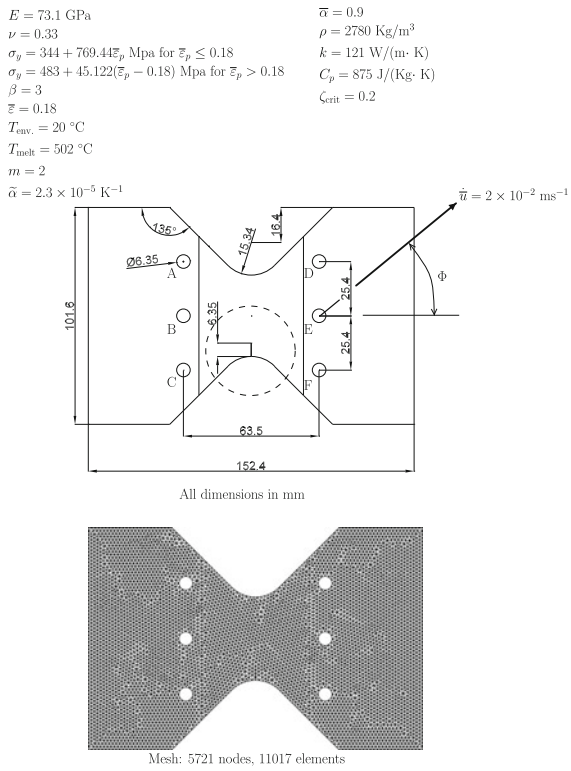

Fig. 12 The Arcan set-up (*top*) and mesh (*bottom*) and all values of the material and model parameter as based on Arcan et al. (1978); Sutton et al. (2000)

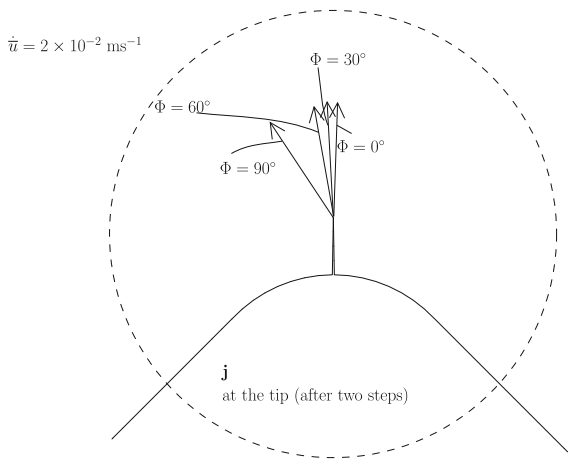

Fig. 13 Configurational forces after 2 time steps in the Arcan test

Further details concerning this topic can be consulted in Areias et al. (2011b). Simulation results of thickness variation are shown in Fig. 15. Corresponding velocity profiles at the crack tip are shown in Fig. 16.

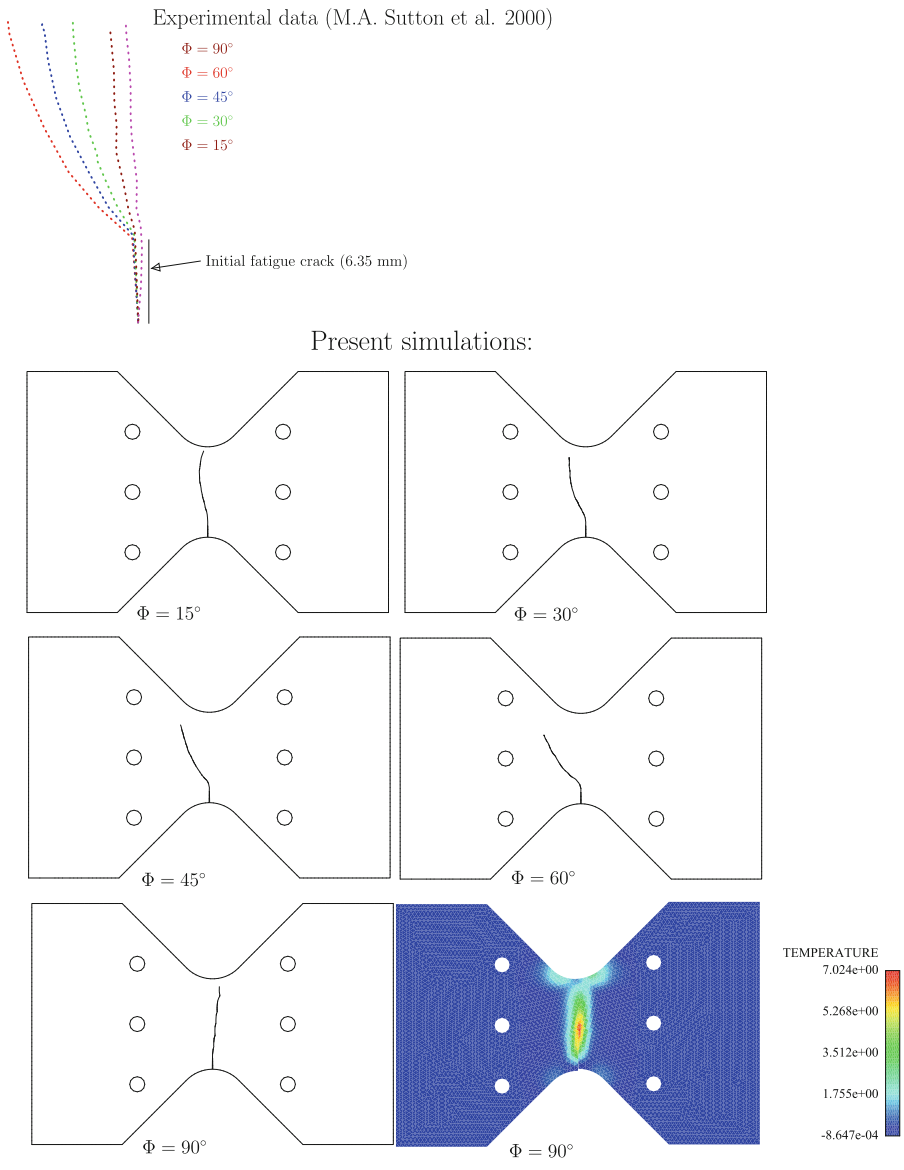

Fig. 14 The crack paths provided by our model as based on configurational forces. The time increment is here 0.1 s

5.4 Force-free elasto-plastic fracture

Crack opening by pure cooling can also be simulated with our method. Heat is flowing throughout the horizontal faces, while no forces are exerted on the boundary. The time increment is here 1.5 s. The crack path is determined by the tip traction by means od (2.17), where the dependence of $\mathbf{P}$ on the temperature is explicitly provided by the formula $\mathbf{P} = \boldsymbol{\tau}\mathbf{F}^{-T}$ with $\boldsymbol{\tau} = \hat{\boldsymbol{\tau}}(\mathbf{b}^{\mathbf{e}}, T)$ given by (3.5). All other field dependence on the temperature are implicitly provided by the flow law, the momentum and the heat equations. Set-up and results are shown in Fig. 17.

Moreover, load-displacement curves are also provided in Fig. 17 for 2 mesh refinements, which are the same as those of Fig. 11.

6 Concluding remarks

The first aim of this paper was to providing a complete fracture simulation model for finite-strain metal

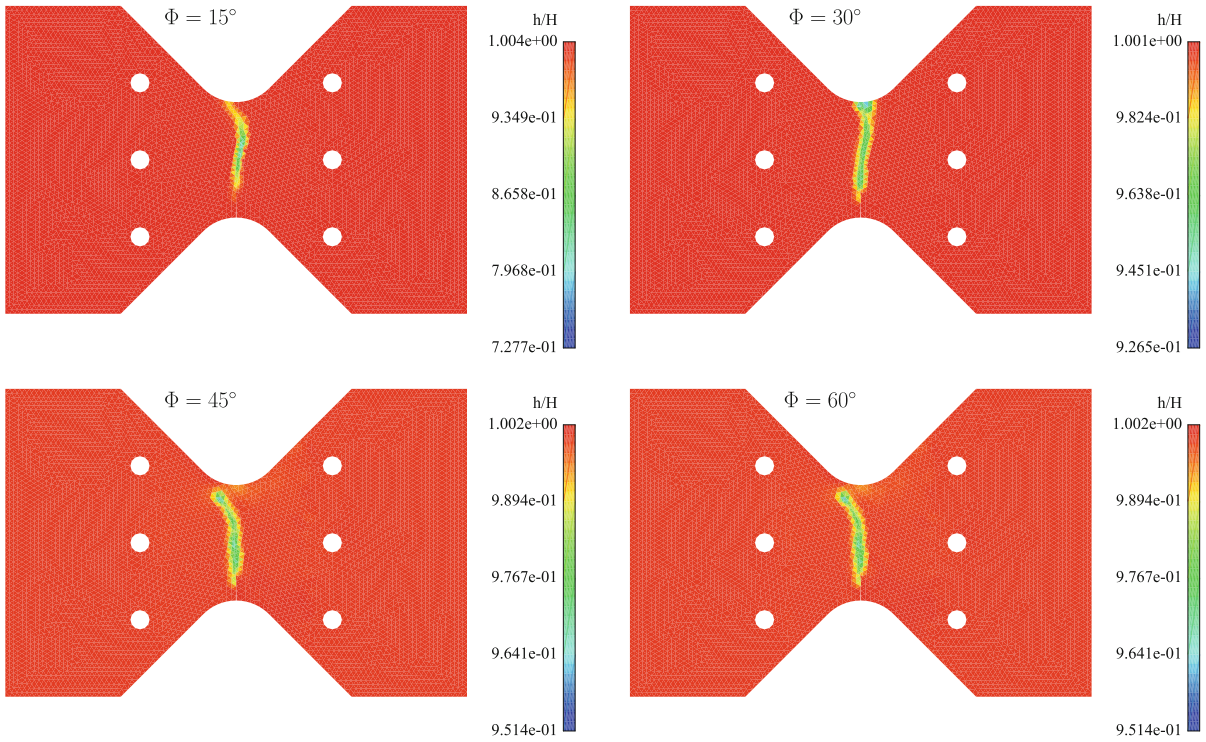

Fig. 15 Thickness variation in the Arcan–Sutton test performed (coarse mesh)

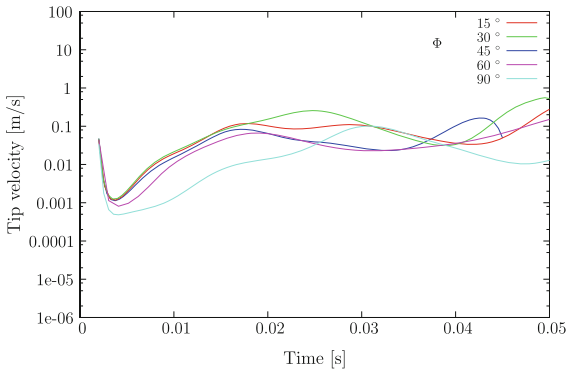

Fig. 16 Crack tip speed as given by Eq. (2.21) in the Arcan–Sutton test with thickness variation (coarse mesh)

plasticity with as few as possible *model parameters*. In total there are 7 parameters, 5 of which are specifically designed for the plastic model, while 2 only are specific for the fracture model. There are 2 parameters in the yield stress expression (3.13), 1 for the damage parameter (3.10), and 1 in the Drucker–Prager equivalent stress (3.15a), while the last plastic parameter is m, the chosen number of plastic surfaces. Concerning crack propagation one needs to provide ζ_{crit}, the chosen threshold for complete softening (at which crack begins to propagate) and R the radius of the contour to compute the crack tip traction in (2.17). In the above simulations the value of R was 1/40th of the body diameter.

The second objective was to be able to justify the model in a deductive manner and this was possible by appealing to Gurtin's notion of *configurational force* (Gurtin 2000). The main interest is then to understand fracture mechanisms, since they follow from rational arguments which can be validated and analyzed by comparing numerical simulation as based on the model with experimental data. This was done in Sect. 5.

Let us also remark that the theory provides an explicit expression of the crack tip speed, which we have features for one simulation example in Fig. 16. To the knowledge of the authors, such an explicit crack tip speed expression in the quasi-static setting is not found in the literature on computational fracture. Let us emphasize that our expression (2.21) comes directly from Gurtin's work (2000), which has served as foundation of our method, model and algorithm.

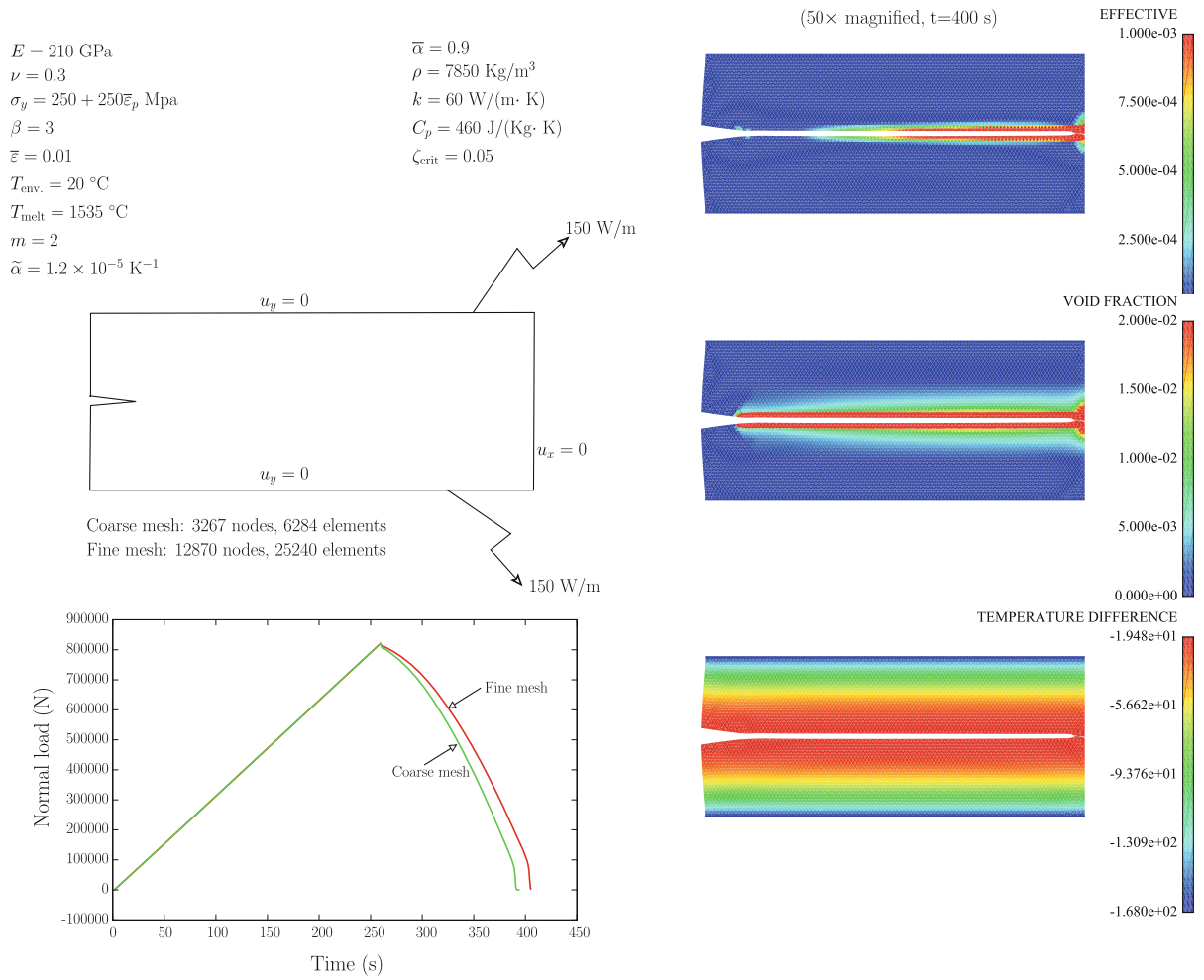

Fig. 17 Crack opening by pure cooling with our model as based on configurational forces

The third goal was to develop a numerical scheme to solve the global problem which is both *nonlinear and non smooth*, cf. Sect. 3. These algorithmic and computational aspects have been less explained in the present paper, since it is based on the SIMPLAS code (https://ssm7.ae.uiuc.edu:80/simplas) whose various ingredients and features have been previously published (Areias and Rabczuk 2010; Areias et al. 2009, 2011b, 2012a.

The present paper then focusses on the two novel aspects of the model, namely the temperature dependence and the crack propagation criterion as based on configurational forces. This latter point is crucial since we believe that its major advantage is its *generality*: a mere modification of the free energy is automatically taken into account in the fracture criterion. For instance if a dislocation model or an electro-magnetic coupling is added to the current thermodynamic model, the specific role played by the dislocations or the Lorentz force on the crack path direction might be accounted for without requiring further ad-hoc procedures. Moreover, as opposed to many other methods based on this notion, here the contour integral is solved directly without need to finely mesh the tip region, which is computationally expensive (and requires to compute the higher order terms).

The specific role of the temperature on crack propagation has also been investigated. Our first concern was to include thermal effects, since temperature is a thermodynamic variable of major importance in every physical mechanism where dissipation plays a crucial role. This is why the temperature appears explicitly or

implicitly in every model equation, including of course in the tip traction expression which determines the kinking direction. Moreover, temperature dependence has been incorporated also because thermal gradients do play a role in the physical mechanisms of fracture. As a matter of fact, our last numerical simulation shows that force-free fracture can also be predicted.

Since the Arcan–Sutton experimental curves have been reproduced with our method (cf. Sect. 5.2) with reasonable accuracy, we believe that our results constitute a solid basis to further analyze fracture, by developing and applying the method to other physical effects. This will be done in future work.

References

Allaire G, Jouve F, Van Goethem N (2011) Damage and fracture evolution in brittle materials by shape optimization methods. J Comput Phys. 33(16):5010–5044

Amstutz BE, Sutton MA, Dawicke DS, Newman JCJr (1995) An experimental study of ctod for mode I/II stable crack growth in thin 2024-t3 aluminum specimens. Fract Mech ASTM, STP 125:256–271

Arcan M, Hashin Z, Voloshin A (1978) A methods to produce uniform plane stress state with applications to fiber-reinforced materials. Exp Mech 18:141–146

Areias P Simplas. https://ssm7.ae.uiuc.edu:80/simplas

Areias P, Belytschko T (2006) Analysis of finite strain anisotropic elastoplastic fracture in thin plates and shells. J Aerosp Eng 19(4):259–270

Areias P, Rabczuk T (2010) Smooth finite strain plasticity with nonlocal pressure support. Int J Numer Method Eng 81:106–134

Areias P, Dias-da-Costa D, Alfaiate J, Júlio E (2009) Arbitrary bi-dimensional finite strain cohesive crack propagation. Comput Mech 45(1):61–75

Areias P, Dias-da-Costa D, Pires EB, Infante Barbosa J (2012a) A new semi-implicit formulation for multiple-surface flow rules in multiplicative plasticity. Comput Mech 49:545–564

Areias P, Rabczuk T, Dias da Costas D, Pires EB (2012b) Implicit solutions with consistent additive and multiplicative components. Finite Elem Anal Des 57:15–31

Areias P, Van Goethem N, Pires EB (2011a) Constrained ale-based discrete fracture in shells with quasi-brittle and ductile materials. In: CFRAC 2011 international conference, CIMNE, Barcelona, June 2011

Areias P, Van Goethem N, Pires EB (2011b) A damage model for ductile crack initiation and propagation. Comput Mech 47(6):641–656

Bai Y, Wierzbicki T (2010) Application of the extended Coulomb–Mohr model to ductile fracture. Int J Fract 161(1–20):157–161

Barenblatt GI (1959) On the equilibrium cracks due to brittle fracture. Doklady AN SSSR 127:47–50 (In Russian)

Bažant ZP (1976) Instability, ductility and size effect in strain softening concrete. J Eng Mech Div-ASCE 102:331–344

Belytschko T, Liu WK, Moran B (2000) Nonlinear finite elements for continua and structures. Wiley, London

Bonet J, Wood RD (2008) Nonlinear continuum mechanics for finite element analysis. 2. Cambridge University Press, Cambridge

Bourdin B, Francfort G, Marigo JJ (2008) The variational approach to fracture. Springer, Berlin

Bourdin B, Larsen CJ, Richardson CL (2011) A time-discrete model for dynamic fracture based on crack regularization. Int J Fract 168(2):133–143

Brezzi F, Fortin M (1991) Mixed and hybrid finite element methods. Springer, Berlin

Chen C, Mangasarian OL (1996) A class of smoothing functions for nonlinear and mixed complementarity problems. Comput Optim Appl 5:97–138

Conti S, de Lellis C (2003) Remarks on the theory of elasticity. Ann Sc Norm Super Pisa, Cl Sci, Ser. 5 2(3):521–549

Crisfield MA, Norris V (1999) A stabilized large-strain elastoplastic $Q_1 - P_0$ method. Int J Numer Method Eng 46:579–592

Doghri I (2000) Mechanics of deformable solids: linear, nonlinear, analytical and computational aspects. Springer, Berlin

Gurtin ME (1981) Topics in finite elasticity. SIAM, Philadelphia

Gurtin ME (2000) Configurational forces as basic concepts of continuum physics. Applied mathematical sciences, vol 137. Springer, Berlin

Gupta A, Markenscoff X (2007) An anisotropic elastic formulation for configurational forces in stress space. Int J Fract 147(1–4):157–161

Gupta A, Markenscoff X (2008) Configurational forces as dissipative mechanisms: a revisit. C R Méc Acad Sci Paris 336(1–2):126–131

James MA, Swenson D (1999) A software framework for two-dimensional mixed mode I/II elastic-plastic fracture. In: Miller KJ, McDowell DL (eds) Mixed mode crack behavior ASTM STP 1359. ASTM International, West Conshohocken

Jirásek M, Bažant ZP (2002) Inelastic analysis of structures. Wiley, London

Klisinski M (1998) On constitutive equations for arbitrary stress-strain control in multi-surface plasticity. Int J Solids Struct 35(20):2655–2678

Korelc J (2002) Multi-language and multi-environment generation of nonlinear finite element codes. Eng Comput 18(4):312–327

Lee EH (1969) Elasto-plastic deformation at finite strains. J Appl Mech ASME 36:1–6

Lemaitre J (1996) A course on damage mechanics, second edition. Springer, Berlin

Li S, Gupta A (2006) On dual configurational forces. J Elast 84(1):13–31

Lubliner J (1990) Plasticity theory. Macmillan, New York

Ma F, Deng X, Sutton MA Jr, Newman JC (1999) Mixed-mode crack behavior, chapter A CTOD-based mixed-mode fracture criterion. Number STP 1359. ASTM American Society for Testing and Materials, West Conshohocken, pp 86–110

Maccagno TM, Knott JF (1992) The mixed mode I/II fracture behavior of lightly tempered hy130 steel at room temperature. Eng Fract Mech 41:805–820

Mandel J (1971) Plasticité classique et viscoplasticité. CISM lecture notes. Springer, Udine

Mattila P (1995) Geometry of sets and measures in Euclidean spaces-fractals and rectifiability. Cambridge studies in advanced mathematics, Cambridge

Maugin GA (1992) The thermomechanics of plasticity and fracture. Cambridge University Press, Cambridge

Mielke A (2003) Energetic formulation of multiplicative elasto-plasticity using dissipation distances. Continuum Mech Thermodyn 15:351–382

Nemat-Nasser S (2004) Plasticity: a treatise on finite deformation of heterogeneous inelastic materials. Cambrige University Press, Cambrige

Oliver J (1995) Continuum modelling of strong discontinuities in solid mechanics using damage models. Comput Mech 17:49–61

Rousselier G, Devaux J-C, Mottet G, Devesa G (1989) Nonlinear fracture mechanics: volume II-Elastic-plastic fracture, chapter "A methodology for ductile fracture analysis based on damage mechanics: an illustration of a local approach of fracture". Number STP 995. American Society for Testing and Materials, Philadelphia, pp 332–354

Simo JC (1988a) A framework for finite strain elastoplasticity based on maximum plastic dissipation and the multiplicative decomposition: part I. Continuum formulation. Comput Method Appl Mech 66:199–219

Simo JC (1988b) A framework for finite strain elastoplasticity based on maximum plastic dissipation and the multiplicative decomposition: Part II. computational aspects. Comput Method Appl Mech 68:1–31

Simo JC, Hughes TJR (1998) Computational inelasticity. Interdisciplinary applied mathematics. Springer, Berlin

Sosa HA, Eischen J (1986) Computation of stress intensity factors for plate bending via a path-independent integral. Eng Fract Mech 25(4):451–462

Sutton MA, Deng X, Ma F, Newman JCJr, James M (2000) Development and application of a crack tip opening displacement-based mixed mode fracture criterion. Int J Solids Struct 37:3591–3618

Truesdell C, Noll W (2004) The non-linear field theories of mechanics. 3. Springer, Berlin

Van Goethem N, Novotny A (2010) Crack nucleation sensitivity analysis. Math Method Appl Sci 33(16):1978–1994

Van Goethem N, Areias P, Pires EB (2011) A temperature-dependent damage model for ductile crack initiation and propagation with finite strains. In: CFRAC 2011 international conference, CIMNE, Barcelona, June 2011

Xue L, Wierzbicki T (2008) Ductile fracture initiation and propagation modeling using damage plasticity theory. Eng Fract Mech 75:3276–3293

Wolfram Research Inc. (2007) Mathematica, Version 6.0, Champaign, IL